Remote Sensing of Suspended Sediments and Shallow Coastal Waters

Rong-Rong Li, Yoram J. Kaufman, Bo-Cai Gao, and Curtiss O. Davis

***Abstract*—Ocean color sensors were designed mainly for remote sensing of chlorophyll concentrations over the clear open oceanic areas (Case 1 water) using channels between 0.4–0.86 μm. The Moderate Resolution Imaging Spectroradiometer (MODIS) launched on the National Aeronautics and Space Administration Terra and Aqua spacecrafts is equipped with narrow channels located within a wider wavelength range between 0.4–2.5 μm for a variety of remote sensing applications. The wide spectral range can provide improved capabilities for remote sensing of the more complex and turbid coastal waters (Case 2 water) and for improved atmospheric corrections for ocean scenes. In this paper, we describe an empirical algorithm that uses this wide spectral range to identify areas with suspended sediments in turbid waters and shallow waters with bottom reflections. The algorithm takes advantage of the strong water absorption at wavelengths longer than 1 μm that does not allow illumination of sediments in the water or a shallow ocean floor. MODIS data acquired over the east coast of China, west coast of Africa, Arabian Sea, Mississippi Delta, and west coast of Florida are used in this study.**

***Index Terms*—Aerosol, remote sensing, ocean.**

I. Introduction

SINCE the launch of the Coastal Zone Color Scanner (CZCS) [6] in 1978, ocean color remote sensing has been focused on the estimation of chlorophyll concentrations over the open oceanic areas (Case 1 water) [10] using satellite instruments having six to eight channels in the spectral range between 0.41–0.865 μm [3], [5]. The main purpose of such remote sensing studies is to improve our understanding of the carbon cycle and the role of the ocean in climate change. In recent years, the ocean science community becomes more interested in remote sensing of the more complex coastal waters. Approximately 60% of the human population lives in the coastal zone. Human activities are modifying the patterns of water runoff and the delivery of nutrients and sediments to coastal waters. The MODIS instrument is a multipurpose instrument with a total of 36 channels for remote sensing of the atmosphere, land surface, and ocean color. In comparison with previous generation of satellite instruments, the MODIS instrument [2], [8], [12] allows improved capabilities for monitoring the more complex and turbid coastal waters (Case 2 water) [10]. In this paper, we describe a simple yet robust algorithm for identifying coastal waters with large amounts of suspended sediments. Shallow coast waters with significant signals reflected from the bottom are also detected. We present sample results from applications of our algorithm to several MODIS datasets acquired over different geographic regions.

Manuscript received June 7, 2002; revised November 24, 2002. This research was supported by the National Aeronautics and Space Administration Goddard Space Flight Center and the Office of Naval Research.

R.-R. Li is with the Science Systems and Applications, Inc., NASA Goddard Space Flight Center, Greenbelt, MD 20771 USA (e-mail: lirongr@climate.gsfc.nasa.gov).

Y. J. Kaufman is with the NASA Goddard Space Flight Center, Greenbelt, MD 20771 USA.

B.-C. Gao and C. O. Davis are with the Remote Sensing Division, Naval Research Laboratory, Washington, DC 20375 USA.

Digital Object Identifier 10.1109/TGRS.2003.810227

II. Background

The impetus to study methods for masking coastal waters was our desire to improve remote sensing of aerosol over the oceans from MODIS [11], [13]. The aerosol retrieving algorithm uses six MODIS channels centered at 0.55, 0.66, 0.86, 1.24, 1.64, and 2.1 μm to derive aerosol models and aerosol optical depths. In the aerosol algorithm, the water leaving radiance is normalized to reflectance units, and called "water leaving reflectance." It is assumed to be zero in the 0.86-, 1.24-, 1.64-, and 2.13-μm channels. The water leaving reflectances at 0.55- and 0.66-μm channels were assumed to be the typical clear water (Case 1) reflectances. Any unaccounted elevated values of the water leaving reflectance were interpreted as an increase in the optical thickness of the fine aerosol particles. Sediments and shallow waters provided such unaccounted high reflectances and resulted in systematic overestimate of the aerosol optical thickness.

In order to improve our aerosol retrieving algorithm over the ocean, we need to develop a procedure to automatically mask out the turbid water areas. Through studies of apparent reflectance spectra acquired with the Airborne Visible Infrared Imaging Spectrometer (AVIRIS) [14] from a NASA ER-2 aircraft at an altitude of 20 km over very turbid waters and relatively clearer waters, as illustrated in Fig. 1, we realized that the main differences between the two types of waters are located in the 0.4–0.7 μm spectral range. The turbid water has significantly larger reflectances than the clear water. This formed the basis for the development of our turbid water masking algorithm for MODIS data. The well-known "apparent reflectance (ρ)" of a given channel is traditionally defined as

$$\rho = \frac{\pi L}{\mu_0 E_0} \tag{1}$$

where L is the measured radiance of the channel, μ_0 the cosine of solar zenith angle, and E_0 the extraterrestrial solar flux.

III. Algorithm

The seven MODIS solar channels centered at 0.47, 0.55, 0.66, 0.86, 1.24, 1.64, and 2.13 μm were originally designed for re-

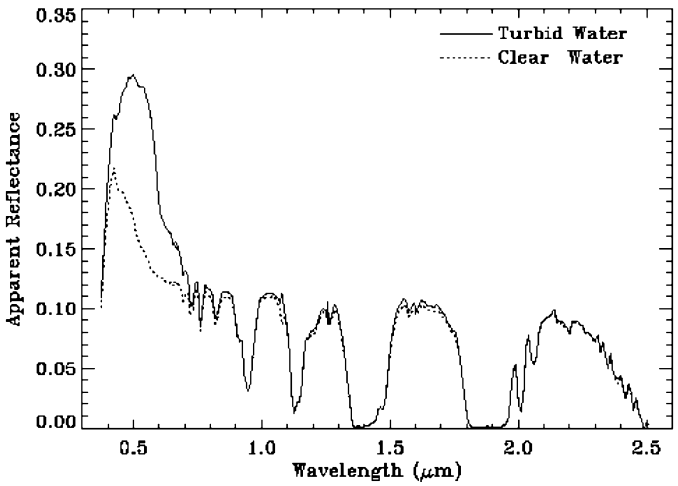

Fig. 1. Examples of apparent reflectance spectra acquired with the Airborne Visible Infrared Imaging Spectrometer (AVIRIS) from a NASA ER-2 aircraft at an altitude of 20 km over the very turbid water (solid line) and relatively clearer water (dotted line). The AVIRIS data were measured over water surfaces close to the Honolulu airport in April 2000.

mote sensing of land and cloud properties [7], [8]. We have found that these channels are quite useful for remote sensing of the brighter coastal waters. In this paper, we describe the algorithm development through examples. Fig. 2 shows a color image (red: 0.66 μm; green: 0.55 μm; blue: 0.47 μm) processed from the MODIS data acquired over the east coastal areas of China on November 11, 2001. Some of the areas were covered by turbid waters with significant amounts of suspended sediments (yellowish color). Portions of the areas were covered by haze aerosol from urban pollution. We selected ten small areas, as marked in the figure, for detailed analysis. Based on visual inspection areas 1 to 5 are less turbid and are referred to here as the "clear" water areas. Areas 6 to 10 are visually turbid water areas with suspended sediments.

The comparisons between the spectral properties of regions with and without sediments are shown in Fig. 3. Fig. 3(a) shows a plot of the ocean + atmosphere reflectance (termed apparent reflectance) as a function of wavelength for clear water from areas 4 and 5. Note that area 4 is influenced more by the haze aerosol than area 5. The spectral reflectances from area 4 fit very well with a power law formula, which is illustrated by a straight line on this log–log scale plot. The same is true for the reflectances from target 5, but with lower values and a steeper slope, due to the smaller aerosol concentration. The correlation for both areas 4 and 5 is 0.999. Fig. 3(b) shows a similar plot for the turbid water areas 8 and 9. A fit was performed using the area 9 data points from the 0.47-, 1.24-, 1.64-, and 2.13-μm channels. Because the reflectances at 0.55-, 0.66-, and 0.86-μm channels are affected by the presence of sediments, the data points from these three channels are not included in the fitting. The observed reflectance values of these three channels are well above the straight line. The excess reflectances are attributed to the back scattering of solar radiation by sediments.

In order to have more theoretical understanding on the usefulness of the longer MODIS wavelengths to separate sediments from aerosol, we have made calculations of pure liquid water transmittance as a function of wavelength using the liquid water

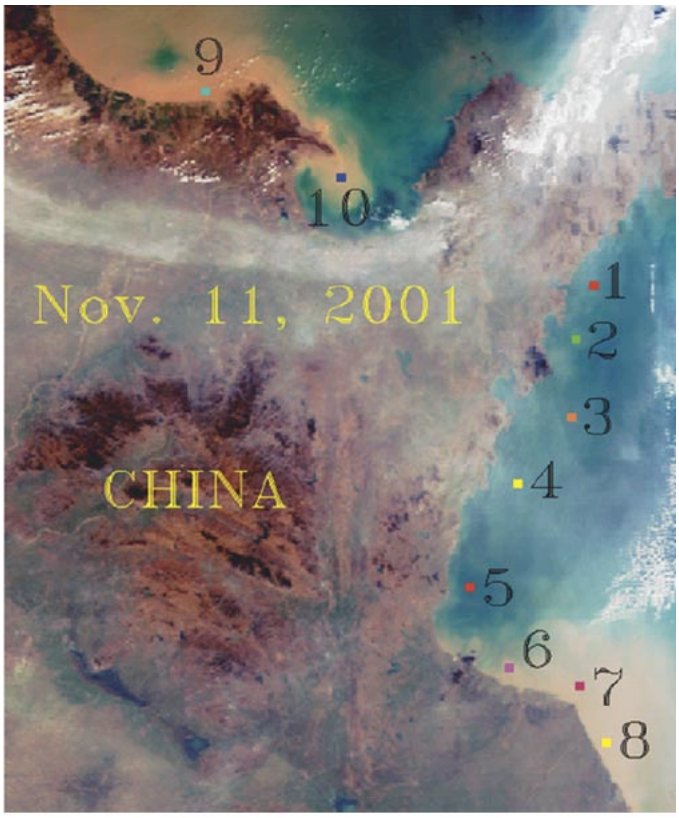

Fig. 2. MODIS image (red: 0.66 μm; green: 0.55 μm; blue: 0.47 μm) acquired over the east coastal areas of China on November 11, 2001. The image shows low sediment areas (1–5), high sediment areas (6–10), and varying amount of pollution aerosol—the gray-brown haze.

absorption coefficients compiled by Wieliczka *et al.* [15]. The transparency of pure water to sunlight decreases rapidly with increasing wavelength in the 0.5–2.5 μm spectral region. Table I lists the penetration depths at the level of 90% light attenuation. The sunlight at 0.55 μm can penetrate about 40 m under the very clear water surface. Its penetration depth is about 50 cm at 0.86 μm, down to 2 cm at 1.24 μm, and further down to 1 mm at 2.13 μm. Thus, the turbidity in water can affect reflectance in visible channels and even at 0.86 μm. It is not easy to distinguish sunlight reflected by turbid waters or by aerosols using wavelengths <1 μm. However, for the longer wavelengths (1.2, 1.6, and 2.1 μm) the penetration depths of sunlight into the water are very small, eliminating the possibility of the reflection by sediments. We found that the blue channel (0.47 μm) is very sensitive to atmospheric molecular scattering, but less sensitive to the additional reflection by sediments. For coastal waters, this channel is not nearly as sensitive as the 0.55-μm channel to sediment reflection because of strong absorption by dissolved organic matters (yellow substances) at 0.47 μm. In summary, the MODIS measurements over the ocean at 0.47-, 1.2-, 1.6-, and 2.1-μm are influenced mainly by aerosol scattering and absorption and can be used to derive the atmospheric spectral power law. Measurements at 0.55–0.86 μm are influenced both by the aerosol and the sediments. The excess reflectance at 0.55–0.86 μm beyond the power law values can be associated to the presence of sediments and used for their detection.

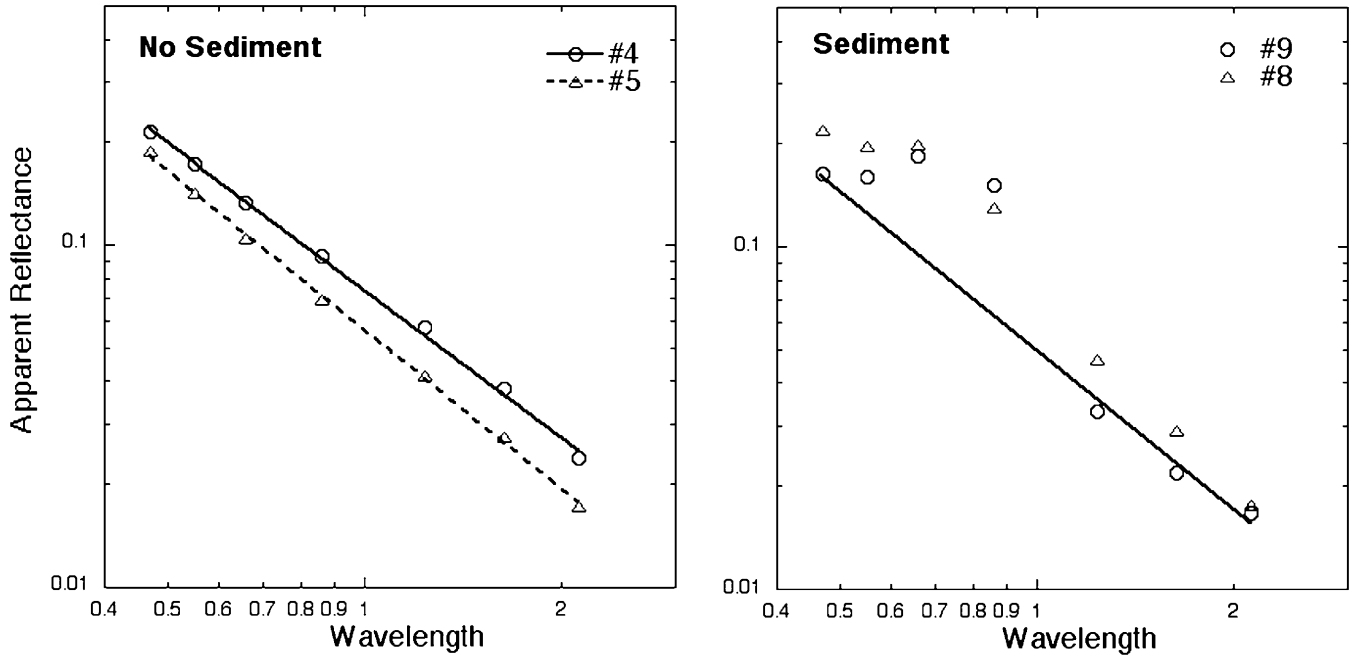

Fig. 3. (a) Plot of the apparent reflectance (reflectance of the ocean + atmosphere) as a function of wavelength for clear water (areas 4 and 5, marked in Fig. 2) and (b) similar plot but for the turbid water areas 8 and 9, as marked in Fig. 2. The line in (b) was obtained using the area 9 data points from the 0.47-, 1.24-, 1.64-, and 2.13-μm channels.

TABLE I
LIGHT PENETRATION DEPTHS AT THE LEVEL OF 90% LIGHT ATTENUATION FOR SEVERAL WAVELENGTHS

Wavelength (μm)	Penetration Depth (m)
0.55	41
0.86	0.49
1.24	0.02
1.64	0.004
2.13	0.001

The sediment masking algorithm follows: we first use the apparent MODIS reflectances at 0.47, 1.24, 1.64, and 2.13 μm to derive the power law fit illustrated in Fig. 3(b). Then we calculate reflectances at 0.55, 0.66, and 0.86 μm based on the fitted line. The differences $\Delta\rho$ between the satellite-measured reflectances of the 0.55-, 0.66-, and 0.86-μm channels and the calculated reflectances for the same channels are the excess reflectance introduced by sediments. Fig. 4 shows the reflectance differences for the 0.55- and 0.66-μm channels and for all the ten selected targets. For the clear water areas, the differences at 0.55 μm are close to zero; while for the turbid water areas, the differences are all greater than 0.01. In this case study, both the 0.55-μm channel and the 0.66-μm channel can, in principle, be used for sediment detections. Our analysis of MODIS data measured over other geographical regions have shown that the reflectance difference for the 0.55-μm channel is also sensitive for detecting shallow waters with bottom reflections. The 0.55-μm channel can sense far deeper into the ocean than the 0.66-μm channel because of much smaller liquid water absorption at 0.55 μm than at 0.66 μm [9]. The shallow waters with measurable bottom reflections also need to be masked out for the aerosol retrievals from MODIS data [13]. Therefore, we have decided to use the reflectance difference of the 0.55-μm channel for sediment masking. The selected threshold value for the reflectance difference is 0.01.

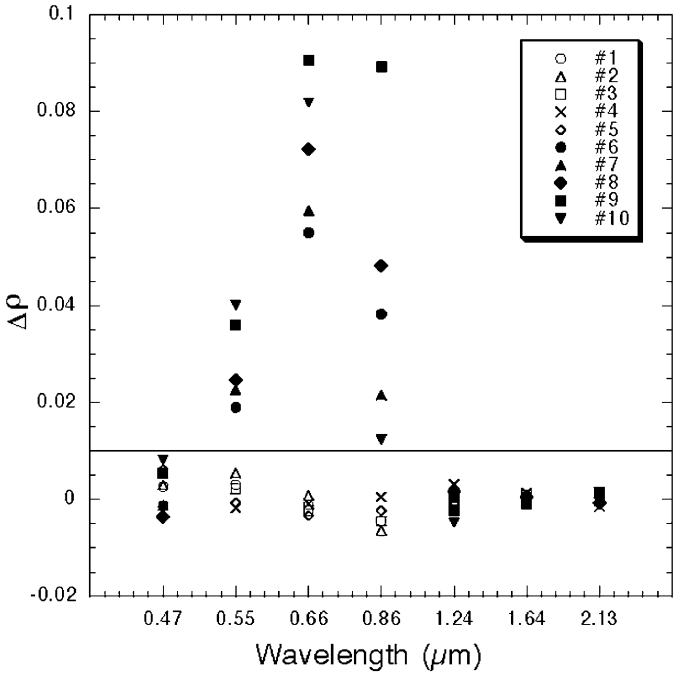

Fig. 4. Reflectance differences for the 0.47-, 0.55–, 0.66-, and 2.13-μm channels for all the ten selected targets marked in Fig. 2. The reflectance difference is calculated as the difference between the actual reflectance measured at the top of the atmosphere and the power law interpolated reflectance (linear fit in a $\log \times \log$ scale). The line at 0.01 is the threshold value used to identify the pixels with high sediment reflectance for masking.

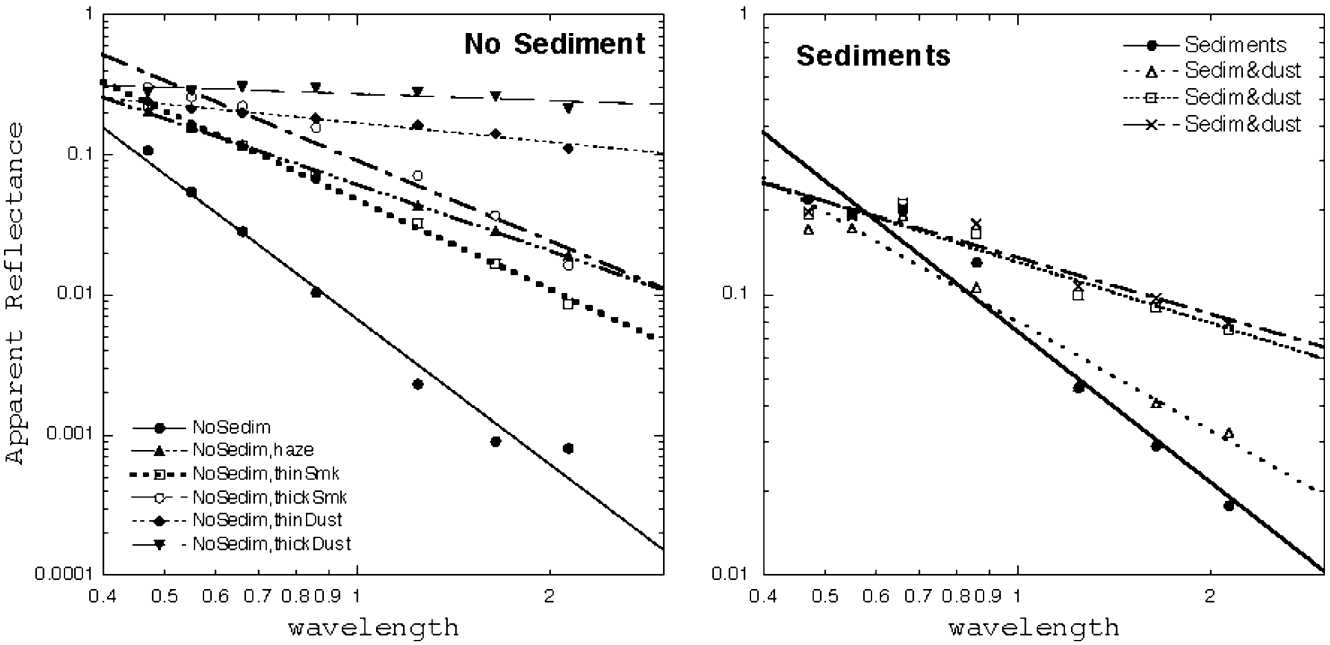

(a) (b)

Fig. 5. (a) Wavelength dependences of MODIS data measured over clear waters and under different atmospheric conditions, such as those with heavy haze, light and heavy smoke, light and heavy dust and (b) similar to (a) but for MODIS data acquired over ocean areas with sediments and under varying atmospheric dust concentrations.

In order to develop an empirical algorithm for global applications, we have examined reflectance properties of different types of targets from many MODIS datasets. Fig. 5(a) shows the wavelength dependences of MODIS data measured over clear waters and under different atmospheric conditions, such as those with large amount of haze, light and heavy smoke originated from biomass burning, light and heavy dust. The absolute reflectance values can differ significantly from one area to another area. However, the data points from the seven MODIS channels for each of the selected areas can be fitted well by a power law (correlation of 97% to 100%) except for very heavy dust where the correlation is only 72%. The reason for the good fit is that aerosol scattered light exhibits a power law dependence to a first degree of approximation. Second order deviations are found for very heavy concentration of specific aerosol types (e.g., dust, smoke, or pollution) [1].

Fig. 5(b) shows MODIS data acquired over areas with sediments and under varying dust conditions. For each of the selected targets, a straight line is obtained by fitting reflectances only from the 0.47-, 1.24-, 1.64-, and 2.13-μm channels. The data points for the measured reflectances of the 0.55-, 0.66-, and 0.86-μm channels are all located above the fitted line. The differences between the measured reflectances for the three channels and those predicted with the straight line result from the scattering of solar radiation by sediments on or below the water surfaces.

We have analyzed more than 30 MODIS datasets acquired over different geographical locations and under varying atmospheric conditions from very clear to heavy smoke or heavy dust. Fig. 6 shows results for the 0.55-μm channel reflectance differences, $\Delta\rho(0.55\ \mu\mathrm{m})$, for many clear water areas and turbid water areas having large amounts of sediments. Most of the clear water areas (open circle) have $\Delta\rho(0.55\ \mu\mathrm{m})$ of 0.01 or less, while most of the turbid water areas (filled triangle) greater

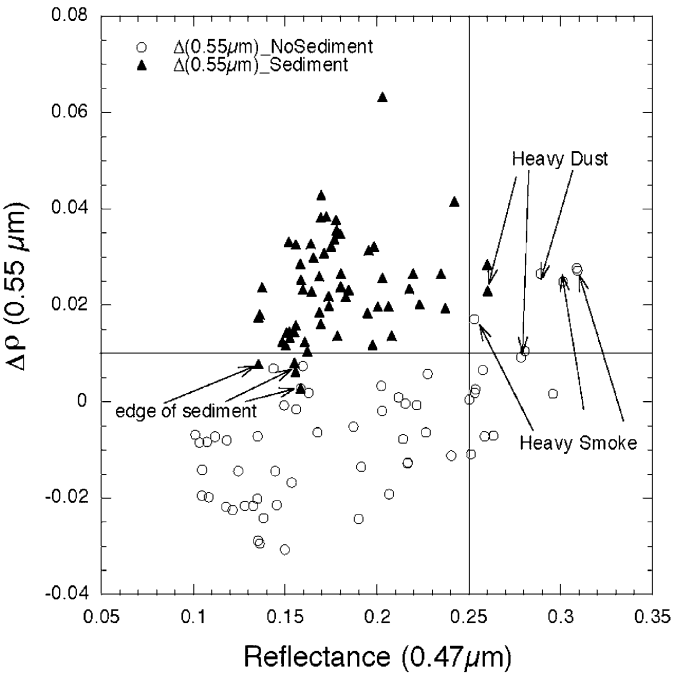

Fig. 6. The 0.55-μm channel reflectance differences for many clear water areas and turbid water areas having large amounts of sediments. The heavy smoke and heavy dust pixels above the 0.01 threshold value were reclassified as nonsediment pixels based on their high reflectance values at 0.47 μm.

than 0.01. There are only a few exceptions. For example, some of clear water areas with heavy smokes or heavy dusts have $\Delta\rho(0.55\ \mu\mathrm{m})$ values greater than 0.01. These areas would be classified as sediment areas based only on the $\Delta\rho(0.55\ \mu\mathrm{m})$ threshold value selected above. In order to avoid this type of misclassifications, we have developed another threshold to deselect these heavy dust or heavy smoke areas. If $\rho(0.47\ \mu\mathrm{m}) >$

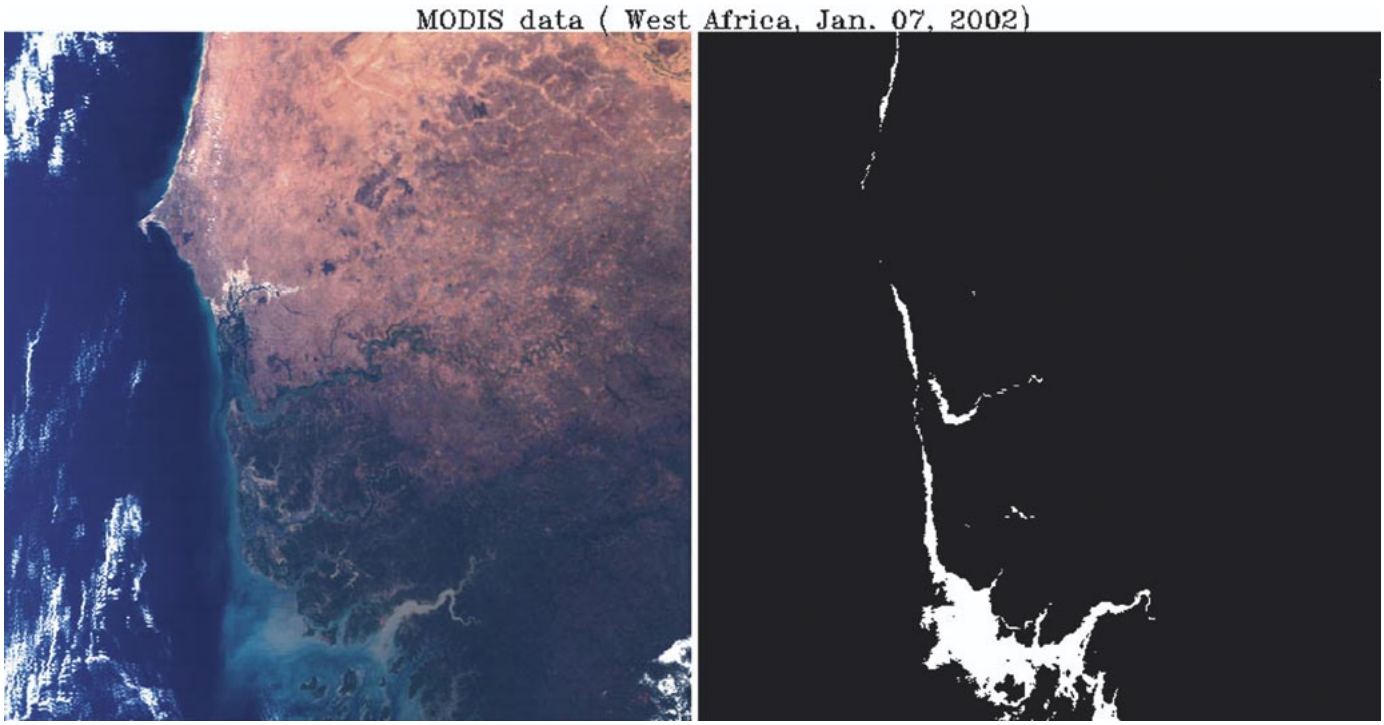

(a) (b)

Fig. 7. (a) MODIS color image (red: 0.66 μm; green: 0.55 μm; blue: 0.47 μm) acquired on January 7, 2002 over the west coastal areas of Africa. (b) Corresponding sediment and shallow water mask image.

0.25, heavy dust or heavy smoke are possible, and the area will not be considered as sediment area. After applying the two thresholds to each pixel in MODIS images, the resulting masks appear to be quite reasonable.

IV. Sample Results

The empirical algorithm described above has been applied to numerous MODIS datasets. Sample results from the data acquired over the west coast of Africa, Arabian Sea, Mississippi Delta, and west coast of Florida are described below. Figs. 7(a), 8(a), 9(a), and 10(a) are all processed from the MODIS channels at 0.66 μm (red), 0.55 μm (green), and 0.47 μm (blue). Figs. 7(b), 8(b), 9(b), and 10(b) are sediment/bottom mask images derived from the MODIS datasets using our algorithm.

A. Western Africa

Fig. 7(a) shows a MODIS image acquired on January 7, 2002 over the west coastal areas of Africa. The image covers roughly the latitude range of 11°N–16°N and the longitude range of 10°W–18°W. The left portion of the image is the Atlantic Ocean. The upper middle and right portions are desert areas. The lower middle and right portions are tropical areas. Fig. 7(b) shows our sediment mask image. Narrow stripes over the coastal waters and rivers are picked out. Large areas with significant amount of sediments from a river discharge near the bottom part of the image are also well identified.

B. Arabian Sea

Fig. 8(a) shows a color image processed from the MODIS data collected over the Arabian Sea and nearby areas on October 28, 2001. The image covers approximately the latitude range of 20°N–25°N and the longitude range of 65°E–73°E. The Gulf of Kutch is seen in the middle portion of this image. The city of Karachi, Pakistan is located near the tip in the upper left portion of the image. Fig. 8(b) shows the sediment mask image. Our masking algorithm has successively picked up turbid water areas seen in Fig. 8(a).

C. Mississippi Delta

Fig. 9(a) shows a color image processed from the MODIS data measured over the southern part of United States and the Gulf of Mexico on March 5, 2001. The image covers approximately the latitude range of 28°N–31°N and the longitude range of 87°W–94°W. Fig. 9(b) shows the sediment mask image. The large bluish and brownish water areas in Fig. 9(a) are properly masked as sediment areas in Fig. 9(b). For example, the areas near the Mississippi River discharge region in the lower right portion of Fig. 9(a) are masked as sediment areas in Fig. 9(b). Mobile Bay, its outflow plume, and the adjacent sound near the upper right corner of Fig. 9(a) are also masked as high sediment areas.

D. West Coast of Florida

Fig. 10(a) shows a color image processed from the MODIS data measured over the southeastern part of United States on March 7, 2001. The image covers roughly the latitude range of 24°N–30°N and the longitude range of 80°W–85°W. Fig. 10(b) shows the sediment/bottom mask image. Large portions of shallow water areas with measurable bottom reflections along the west coast of Florida are picked in the masking image.

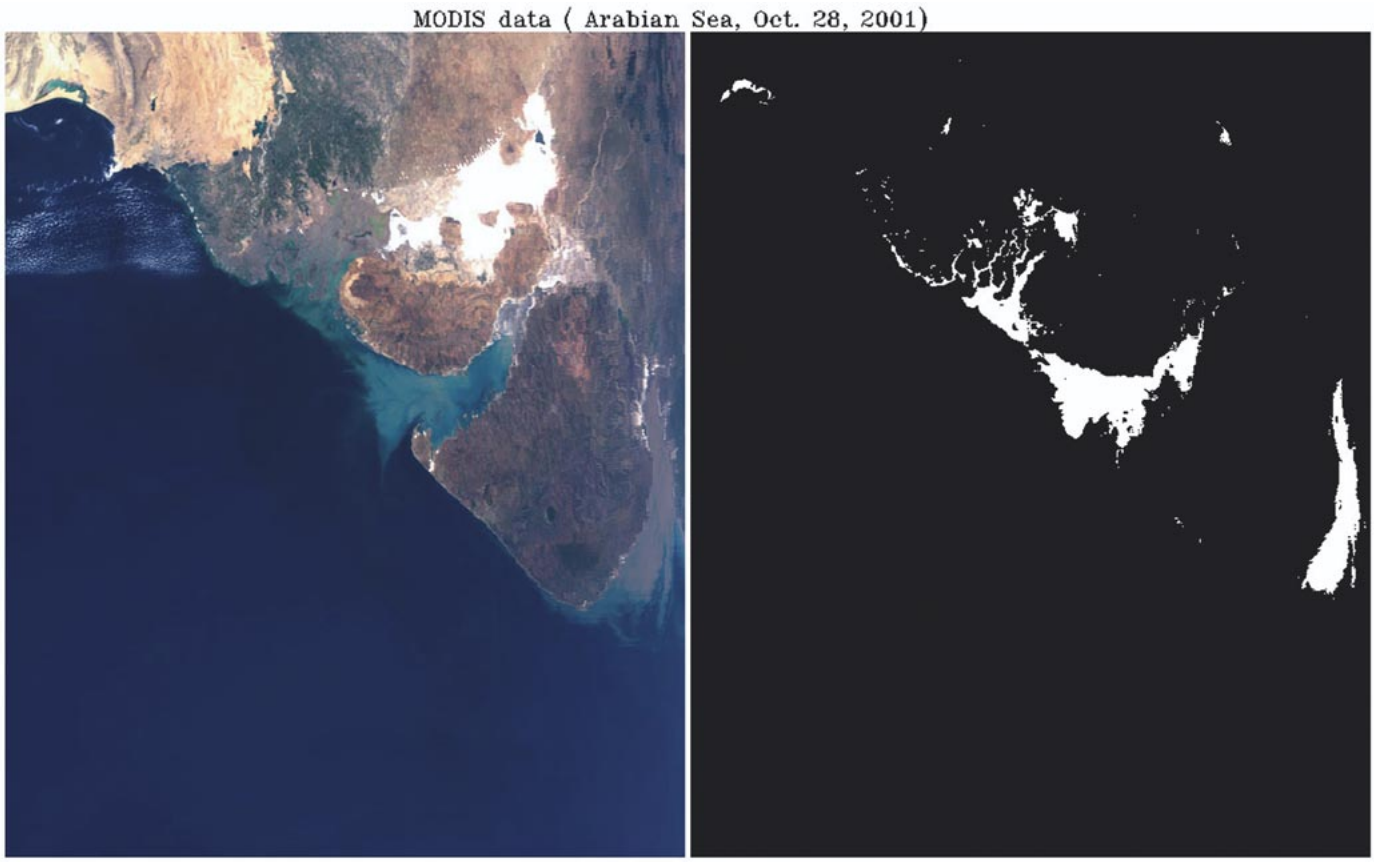

(a) (b)

Fig. 8. (a) Color image processed from a MODIS dataset collected over the Arabian Sea and nearby areas on October 28, 2001. (b) Corresponding sediment and shallow water mask image.

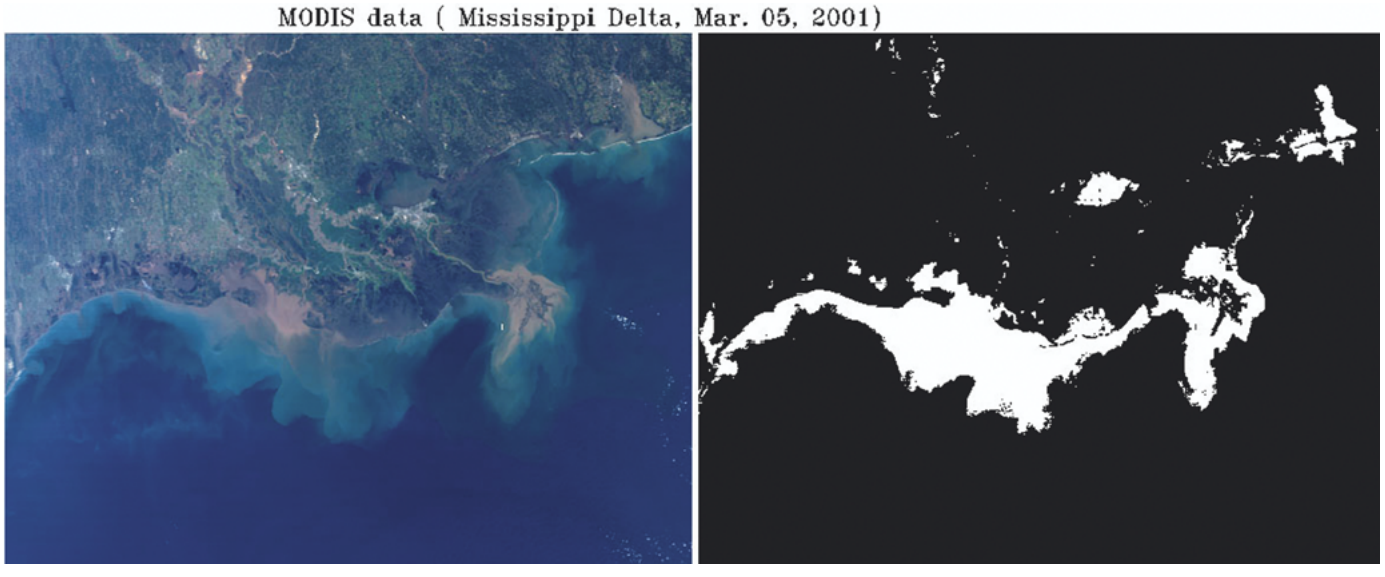

(a) (b)

Fig. 9. (a) Color image processed from a MODIS dataset measured over the southern part of United States and the Gulf of Mexico on March 5, 2001. (b) Corresponding sediment and shallow water mask image.

V. Discussion

Traditionally, the detection of ocean color was done using only channels with wavelengths shorter than 0.86 μm and mainly applied for remote sensing of Case 1 water. Meanwhile, the MODIS channels at 1.2–2.1 μm were found to be very useful for remote sensing of aerosol, in particular that of supermicron dust and sea salt particles. These channels are located in a spectral region with strong liquid water absorption, and therefore can measure aerosol scattering independent of the

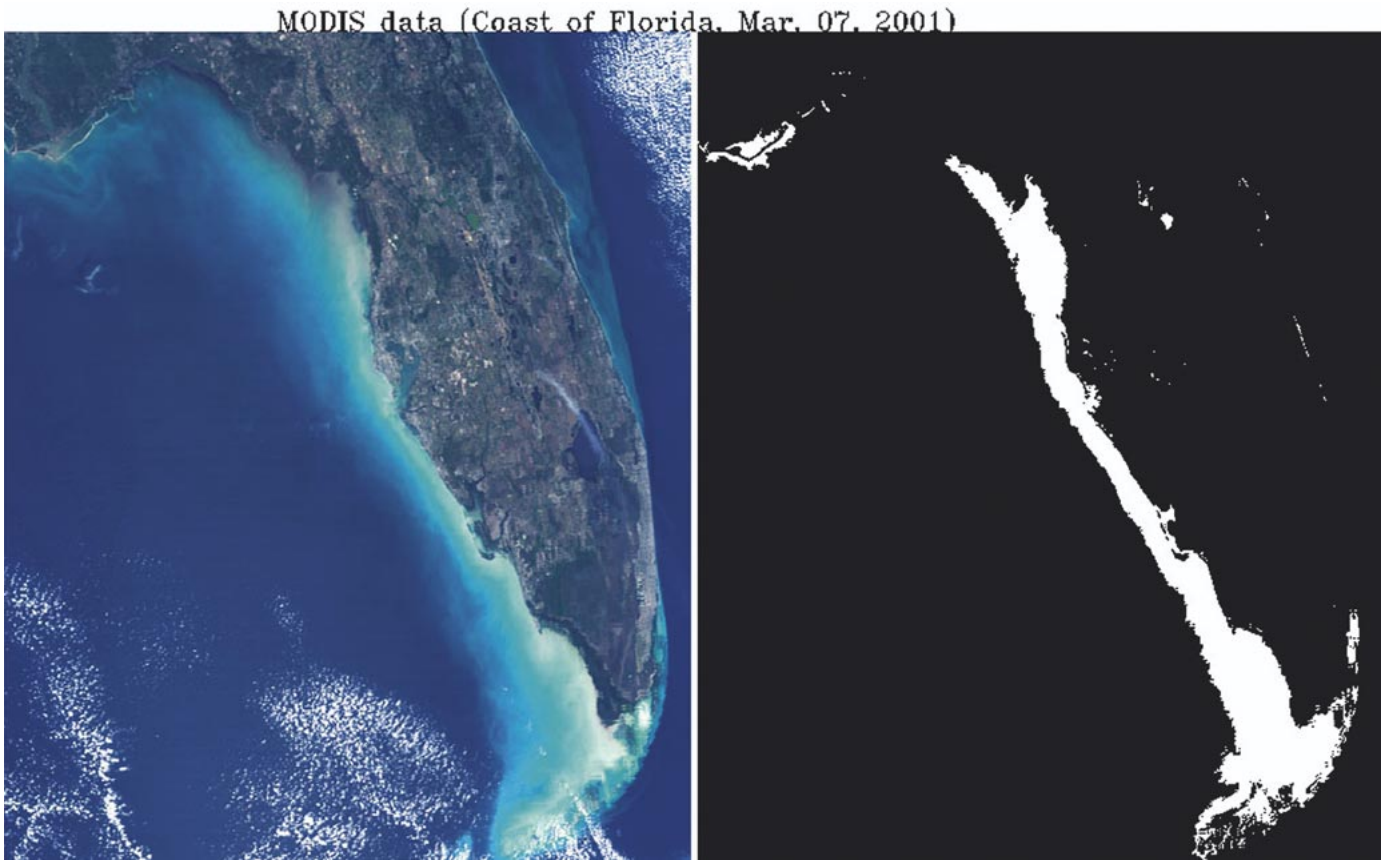

(a) (b)

Fig. 10. (a) Color image processed from a MODIS dataset collected over the southeastern part of United States on March 7, 2001. (b) Corresponding sediment and shallow water mask image.

turbidity of ocean waters and other properties. Using the spectral characteristics of these channels, an empirical algorithm for masking sediment and shallow water areas was developed. We have used three MODIS channels at longer wavelengths (1.24, 1.64, and 2.13 μm) in addition to the 0.47-μm channel to define a power law baseline atmospheric reflection level. Sediments and shallow waters are masked as excess reflectance at 0.55-μm above the power law reflectance. The algorithm described here for identifying areas with suspended sediments in turbid waters and shallow waters with bottom reflections works fine under most atmospheric conditions with low to moderate aerosol loadings. Under the very hazy conditions when the surface radiances in the visible are completely blocked out by aerosols in the upward paths, the MODIS instrument will not be able to see surface features in the visible channels, and our algorithm will not be useful for sediment detections.

It should be pointed out that the MODIS instrument has a set of highly sensitive narrow channels designed specifically for remote sensing of the clear deep ocean waters and located in the wavelength range between 0.41–0.86 μm [4], [8]. Over the bright coastal waters, quite a few of these ocean color channels can be saturated because of too much radiance reaching the relevant detectors. To avoid this problem, we have used only the seven land and cloud channels for this algorithm.

The algorithm described in this paper is mainly designed for masking out all bright pixels in coastal water areas so that these pixels will not be used during the retrievals of aerosol information from MODIS data. We mask out pixels with high sediment reflectances and shallow water pixels with detectable bottom reflections using the 0.55-μm channel reflectance differences. During the study, we noticed that it may be possible to develop more refined algorithms to separate sediment areas from shallow water areas using a combination of reflectance differences of the 0.55-μm, 0.66-μm, and 0.86-μm channels, each with a different penetration depth (see Table I). The 0.66-μm and 0.86-μm channels receive little radiances resulting from the bottom reflection because of the increased liquid water absorption [9]. Unlike Case 1 waters, Case 2 waters are located in well-defined geographical regions. The sources of sediments from river runoff are generally known. The spectral properties of these sediments can be measured during field experiments. It may be possible to develop further refined region-specific empirical algorithms for remote sensing of sediments and shallow waters from MODIS data.

VI. Summary

In order to improve the MODIS operational aerosol retrieving algorithm, we have developed a simple and robust method using a set of MODIS land and cloud channels in the visible and near-infrared spectral region for identifying coastal waters with significant amounts of suspended sediments and shallow waters with detectable bottom reflections. The method is developed based on the analyses of many MODIS datasets measured

under different atmospheric conditions. Quite reasonable results have been obtained when the method is applied to full MODIS imaging datasets acquired over different geographical regions in the globe.

ACKNOWLEDGMENT

The authors are grateful to W. Esaias (NASA Goddard Space Flight Center) for useful discussions.

REFERENCES

[1] T. F. Eck, B. N. Holben, O. Dubovik, A. Smirnov, I. Slutsker, J. M. Lobert, and V. Ramanathan, "Column-integrated aerosol optical properties over the Maldives during the northeast monsoon for 1998–2000," *J. Geophys. Res.*, vol. 106, pp. 28 555–28 566, 2001.

[2] W. E. Esaias, M. R. Abbott, I. Barton, O. B. Brown, J. W. Campbell, K. L. Carder, D. K. Clark, R. H. Evans, F. E. Hoge, H. R. Gordon, W. M. Balch, R. Letelier, and P. J. Minnett, "An overview of MODIS capabilities for ocean science observations," *IEEE Trans. Geosci. Remote Sensing*, vol. 36, pp. 1250–1265, July 1998.

[3] H. R. Gordon, D. K. Clark, J. L. Mueller, and W. A. Hovis, "Phytoplankton pigments derived from the Nimbus-7 CZCS: Initial comparisons with surface measurements," *Science*, vol. 210, pp. 63–66, 1980.

[4] H. R. Gordon, "Atmospheric correction of ocean color imagery in the earth observing system era," *J. Geophys. Res.*, vol. 102, pp. 17 081–17 106, 1997.

[5] S. B. Hooker, W. E. Esaias, G. C. Feldman, W. W. Gregg, and C. R. McClain, "An Overview of SeaWiFS and Ocean Color," NASA, Greenbelt, MD, Tech. Memo. 104 566, ser. SeaWiFS Technical Report Series, vol. 1, 1992.

[6] W. A. Hovis, D. K. Clark, F. Anderson, R. W. Austin, W. H. Wilson, E. T. Baker, D. Hall, H. R. Gordon, J. L. Mueller, S. Y. E. Sayed, B. Strum, R. C. Wrigley, and C. S. Yentsch, "Nimbus 7 coastal zone color scanner: System description and initial imagery," *Science*, vol. 210, pp. 60–63, 1980.

[7] C. Justice, E. Vermote, J. Townshend, R. Defries, D. P. Roy, D. K. Hall, V. V. Salomonson, J. Privette, G. Riggs, A. Strahler, W. Lucht, R. Myneni, Y. Knjazihhin, S. Running, R. Nemani, Z. Wan, A. Huete, W. van Leeuwen, R. Wolfe, L. Giglio, J.-P. Muller, P. Lewis, and M. Barnsley, "The Moderate Resolution Imaging Spectroradiometer (MODIS): Land remote sensing for global change research," *IEEE Trans. Geosci. Remote Sensing*, vol. 36, pp. 1228–1249, July 1998.

[8] M. D. King, Y. J. Kaufman, W. P. Menzel, and D. Tanre, "Remote sensing of cloud, aerosol and water vapor properties from the Moderate Resolution Imaging Spectrometer (MODIS)," *IEEE Trans. Geosci. Remote Sens.*, vol. 30, pp. 2–27, Jan. 1992.

[9] C. D. Mobley, *Light and Water Radiative Transfer in Natural Waters*. New York: Academic, 1994, pp. 80–100.

[10] A. Morel and L. Pirieur, "Analysis of variations in ocean color," *Limnol. Oceanogr.*, vol. 22, pp. 709–722, 1977.

[11] L. A. Remer, D. Tanré, Y. J. Kaufman, C. Ichoku, S. Mattoo, R. Levy, D. A. Chu, B. N. Holben, O. Dubovik, A. Smirnov, J. V. Martins, R.-R. Li, and Z. Ahmad, "Validation of MODIS aerosol retrieval over ocean," *Geophys. Res. Lett.*, vol. 29, no. 12, pp. 1–4, 2002.

[12] V. V. Salomonson, W. L. Barnes, P. W. Maymon, H. E. Montgomery, and H. Ostrow, "MODIS: Advanced facility instrument for studies of the earth as a system," *IEEE Trans. Geosci. Remote Sens.*, vol. 27, pp. 145–153, Mar., 1989.

[13] D. Tanré, Y. J. Kaufman, M. Herman, and S. Mattoo, "Remote sensing of aerosol properties over oceans using the MODIS/EOS spectral radiances," *J. Geophys. Res.—Atmos.*, vol. 102, no. D14, pp. 16 971–16 988, 1997.

[14] G. Vane, R. O. Green, T. G. Chrien, H. T. Enmark, E. G. Hansen, and W. M. Porter, "The Airborne Visible/Infrared Imaging Spectrometer," *Remote Sens. Environ.*, vol. 44, pp. 127–143, 1993.

[15] D. M. Wieliczka, S.-S. Weng, and M. R. Querry, "Wedge shaped cell for highly absorbent liquids: Infrared optical constants of water," *Appl. Opt.*, vol. 28, pp. 1714–1719, 1989.

Rong-Rong Li received the B.S. degree in optical physics from Nankai University, Tianjin, China, in 1982, and the M.S. and Ph.D. degrees in physics from the University of Cincinnati, Cincinnati, OH, in 1989 and 1995, respectively.

She is currently with Science Systems and Applications, Inc., NASA Goddard Space Flight Center, Greenbelt, MD. She has conducted research in remote sensing of atmospheric aerosols, water vapor, clouds, vegetation indices, fire, and coastal waters using multispectral and hyperspectral imaging data acquired from both aircraft and satellite platforms.

Yoram J. Kaufman received the B.S. and M.S. degrees in physics from the Technion—Israel Institute of Technology, Haifa, Israel, in 1972 and 1974, respectively, and the Ph.D. degree from Tel-Aviv University, Tel-Aviv, Israel, in 1979.

He came to NASA Goddard Space Flight Center, Greenbelt, MD, in 1979 as an NRC Resident Research Associate. He is currently an Atmospheric Scientist in the Laboratory for Atmospheres, NASA Goddard Space Flight Center. His present research includes theoretical and experimental investigations in atmospheric science, radiative transfer, and remote sensing. His research experience includes remote sensing of aerosols and clouds, atmospheric correction of satellite imagery of the earth's surface, interaction of aerosols with clouds and their subsequent impact on climate, remote sensing of emissions from biomass burning in the topics, and calibration of satellite sensors. He is a member of the MODIS Science Team, where he has primary responsibility for the remote sensing of tropospheric aerosol properties over land surfaces and served as Project Scientist of Terra from 1996 to 2000.

Bo-Cai Gao received the B.S. degree in physics from Nankai University, Tianjin, China, in 1982, and the M.S. and Ph.D. degrees in physics from The Ohio State University, Columbus, in 1984 and 1988, respectively.

He is currently with the Remote Sensing Division, Naval Research Laboratory, Washington, DC. He has been a member of the MODIS Science Team since 1996, where his focus is on the remote sensing of cirrus clouds, atmospheric water vapor, and coastal water.

Dr. Gao received a Prize Paper Award from the IEEE Geoscience and Remote Sensing Society (IGARSS) in 1991 for his development of an operational atmospheric radiative transfer code to retrieve surface reflectance spectra from hyperspectral imaging data measured with the NASA/JPL Airborne Visible/Infrared Imaging Spectrometer (AVIRIS).

Curtiss O. Davis received the B.S. degree in zoology from the University of California, Berkeley in 1966, and the Ph.D. degree in oceanography from the University of Washington, Seattle, in 1973.

He is currently a Senior Scientist for Optical Remote Sensing and is Head of the Optical Sensing Section, Remote Sensing Division, Naval Research Laboratory (NRL), Washington, DC. He was a Program Manager for the National Aeronautics and Space Administration (NASA) Ocean Productivity Program from 1984 to 1986. He was a Research Oceanographer and Group Supervisor of Biological and Polar Oceanography, Jet Propulsion Laboratory (JPL), Pasadena, CA, from December 1986 to March 1994. While at JPL, he was the Project Scientist for the High Resolution Imaging Spectrometer (HIRIS) from July 1990 to March 1994. In 1994, he moved to NRL to develop a program in hyperspectral remote sensing of the coastal ocean. He is a member of the NASA SeaWiFS Science Team and has participated in numerous calibration and validation experiments. He is the Project Scientist for the Navy's Hyperspectral Remote Sensing Technology Program, a focused effort to develop the use of hyperspectral imaging for the characterization of the coastal ocean and to fly the Coastal Ocean Imaging Spectrometer on the Naval EarthMap Observer Satellite.